49

UNIVERSITY OF NEW MEXICO
ALBUQUERQUE

ENGINEERING EXPERIMENT STATION

EP-115

Annual Report
June 1963 to June 1964

MAGNETORESISTANCE, SUPERCONDUCTIVITY AND THE HALL EFFECT FOR INVERTER APPLICATIONS

EP1

By
Richard Bechtel
Sang S. Pak
N. E. Crannemann

UNM

August, 1964

This work performed under
NASA Contract No. NsG 279/62

ENGINEERING EXPERIMENT STATION
The University of New Mexico
Albuquerque, New Mexico

MAGNETORESISTANCE, SUPERCONDUCTIVITY AND THE HALL EFFECT FOR INVERTER APPLICATIONS

Annual Report
June 1963 to June 1964

EE-115

By
Richard Bechtel
Sang So Pak
W. W. Grannemann

August, 1964

This work performed under
NASA Contract No. NsG 279/62

1.0 Introduction

The superconductivity program has been delayed experimentally due to a ten month delay in obtaining a usable liquid helium dewar. When delivery was made in March, it was found that the dewar had several thermal shorts and was completely unusable. It was sent back for complete reconstruction immediately along with a defective liquid helium level indicator. The dewar was returned on June 21 and has been used for two test runs to date. The results are presented herein but are somewhat inconclusive as yet. An addendum to this report will be submitted later on which will include the results and conclusions of future work that is planned.

During the waiting period for the dewar, some attention was diverted to a study of a multi-terminal Hall generator. This study was quite intensive, and some interesting results were uncovered which are described herein. The study included a theoretical development which enables one to optimize parameter values to maximize the generator efficiency.

Also during this interim period, measurements were made on several magnetoresistor configurations at liquid nitrogen temperature. These measurements were made in the defective dewar before it was sent back for reconstruction. At that time the dewar would not hold liquid helium but could be used with liquid nitrogen where boil-off due to thermal-shorts was not as great. However it was necessary to use relatively low magnetic fields since a 1 3/16" pole gap is required for the dewar tailsection.

2.0 Construction of Test Specimens

The following is a discussion of the techniques used in constructing magnetoresistance and superconductive samples. The experimental results for these samples is presented and discussed in the following two sections.

2.1 Magnetoresistance Samples (Fig. 2.1):

All of the samples shown in Figure 2.1 were molded under high vacuum using the apparatus shown in Figure 2.2. The molds were machined out of ultra-high purity carbon with the base block having the sample shape machined into it, and the top block, machined flat to press the molten metal into place. Of course, this apparatus is suitable only for flat samples, but there is no foreseeable need for any type other than this.

The entire apparatus was placed into a vacuum chamber and the heater current kept below that which would cause the metal pellets to melt until out-gassing was complete and a vacuum of 10^{-6} torr was obtained. The samples were allowed to cool sufficiently under vacuum to prevent oxidation.

After the sample was removed from its mold, contacts were soldered on using standard coreless lead-tin solder or indium. Either solder material proved equally successful when copper wire was used. When an attempt was made to use niobium wire[1]

---

[1] This sample was intended to determine the effect of eliminating the IR drop in the circumferential contact of a corbino disk, since Nb is a superconductor.

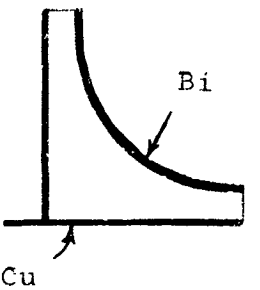

A

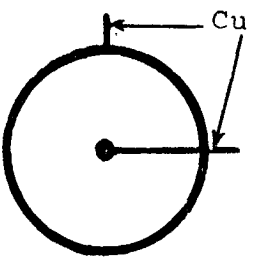

B

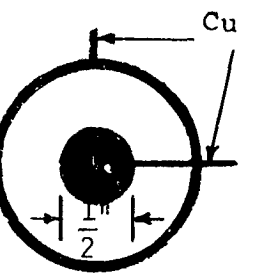

C

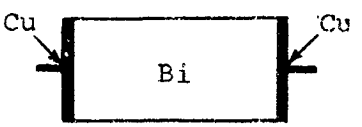

D

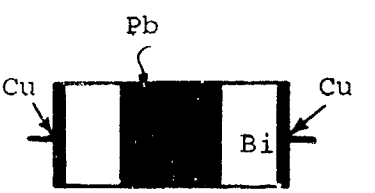

E

Magnetoresistance Samples

Figure 2.1

Molding Apparatus

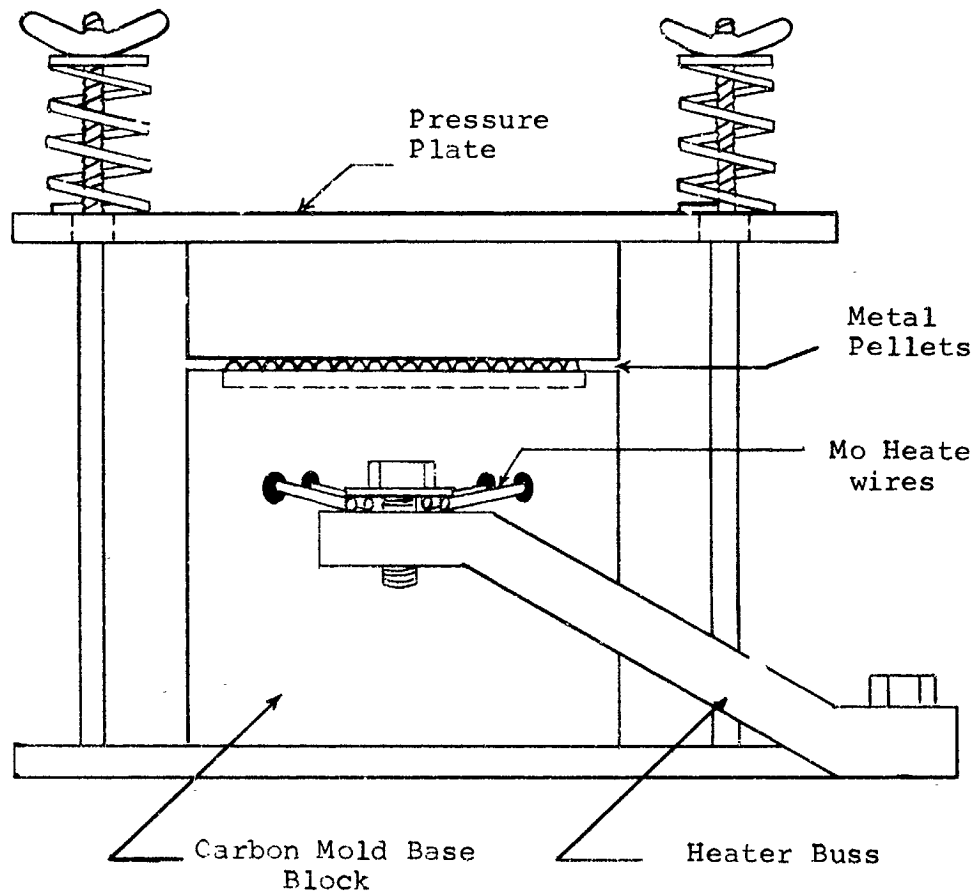

Figure 2.2

for the outer contact on a bismuth corbino disk, no more than a poor and unsuitable physical contact could be obtained because of bonding difficulties inherent with this metal. A search of the metallurgical field revealed that no relatively simple technique is as yet known for bonding a low melting temperature metal to niobium. Therefore, this sample has been abandoned, at least for the time being.

2.2 Superconductivity Samples:

In addition to the superconductivity specimens described earlier,[2] one other has been constructed. This sample is a six foot piece of 20 mil niobium wire which has 500 turns of insulated 20 mil copper wire co-axially wound around it as a field coil. The whole assembly was formed into a two inch diameter coil to fit into the dewar tailsection.

This sample has not been discussed in previous reports and has not yet been tested at liquid helium temperatures; therefore, a discussion of what it is intended for will be included here.

The niobium wire is to be the high current conductor and switch, while the copper winding will produce the control field. There are t' e ways this specimen can function as a switch at $4.2^{\circ}K$: 1) The sample could be placed in a DC magnetic field of a magnitude just less than critical for niobium and then a small AC current applied to the field winding to switch the niobium wire in and out of superconductivity. 2) The current through the

[2] R. Bechtel, W. W. Grannemann, "Magnetoresistance and Superconductivity for Applications for DC to AC Conversion," PR-49, UNM Technical Report.

niobium, while in the superconducting state, could be adjusted to just less than that required to drive the niobium normal (see the discussion of Silsbee's hypothesis[3]) and then switched by a AC current in the field winding. 3) A combination of current, DC magnetic field, and AC field from the field winding. These three methods are sufficient to cover the various requirements that could develop from different applications. That is, a compromise must be made between the desired magnitude of the "on" (superconducting) current and "off" (normal) current, the normal resistance of the superconducting wire, the I^2R losses in producing a DC magnetic field, and the I^2R plus reactive losses and generation losses in producing the AC magnetic field in the field winding. Additional flexibility can be obtained through choice of the superconductive wire from a selection of several that are applicable; e.g., niobium, lead, vanadium, and the various niobium-zirconium alloys.

3.0 Magnetoresistance Measurements at 80°K

The following is a discussion of the experimental results obtained at liquid nitrogen temperature for the bismuth samples shown in Fig. 2.1. All measurements for these samples were made in the special dewar, thus the maximum magnetic field obtainable was 14 kilogauss due to the 1 3/16" gap necessary for the tail-section. None of the measurements indicated complete saturation at this maximum field, however.

---

[3] B. J. Harper, R. Bechtel, W. W. Grannemann, "A Study of the Hall Effect and Magnetoresistance for Low Voltage, High Current, DC to AC Conversion," EE-96, UNM Technical Report.

Sample A:

This sample is the irregular shape magnetoresistor of the type that demonstrated K (magnetoresistance ratio) values nearly on a par with corbino disks when indium antimonide was used at room temperature. This type configuration has a higher current carrying capability than a corbino disk of comparable size. The maximum K value measured was 63.3 at 14 kg. A plot of K versus magnetic field is shown in Fig. 3.1.

Sample B:

This sample is a standard corbino disk of comparable size to sample A. The center conductor diameter is about one millimeter, and the overall diameter about 4 centimeters. A maximum K of 71 was measured at 14 kg. Compare this with the value of 63.3 that was measured for sample A. The difference here is only about 10 percent. However, sample A obviously could handle much larger currents than sample B due to its greater contact area.

A plot of magnetoresistance ratio versus magnetic field is shown in Fig. 3.2. Since this sample demonstrated such good response, it was held over for test runs at liquid helium temperature. These measurements are described in Section 4.

Sample C:

This corbino was constructed in order to determine the effect on the magnetoresistance ratio of increasing the inner conductor diameter. The measurements indicated that the magnetoresistance was drastically decreased by this procedure. This

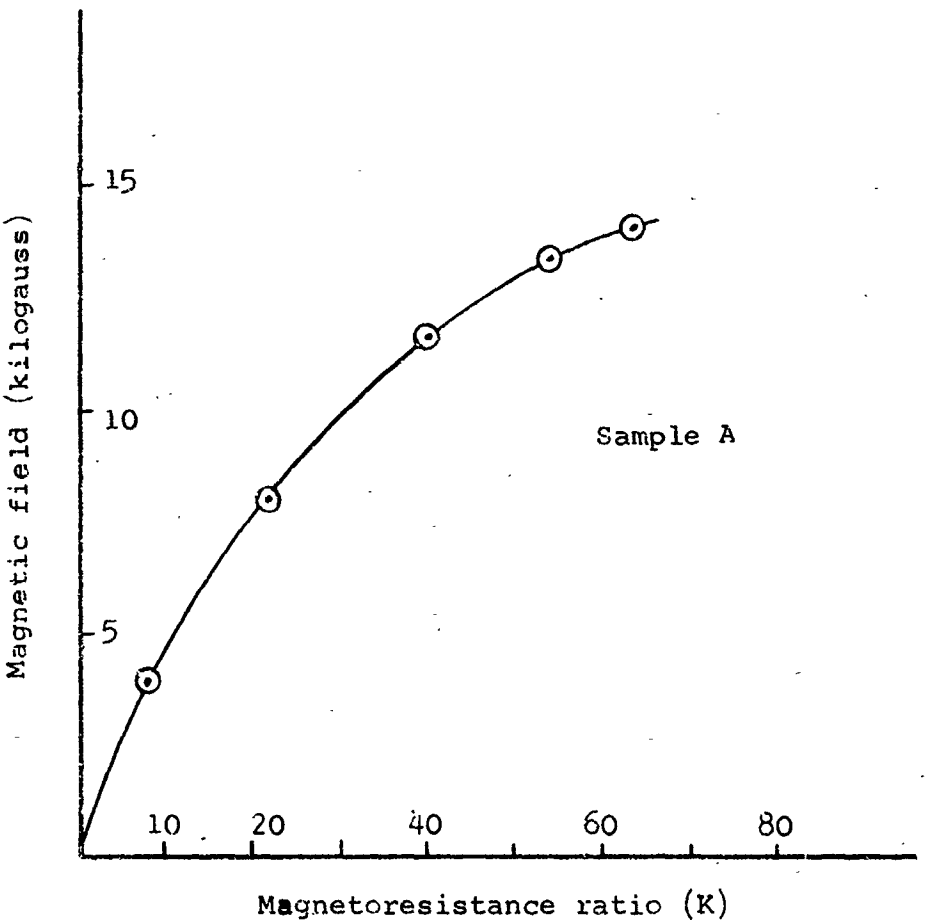
Magnetic field (kilogauss)
15
10
5
Sample A
10
20
40
60
80
Magnetoresistance ratio (K)

Figure 3.1

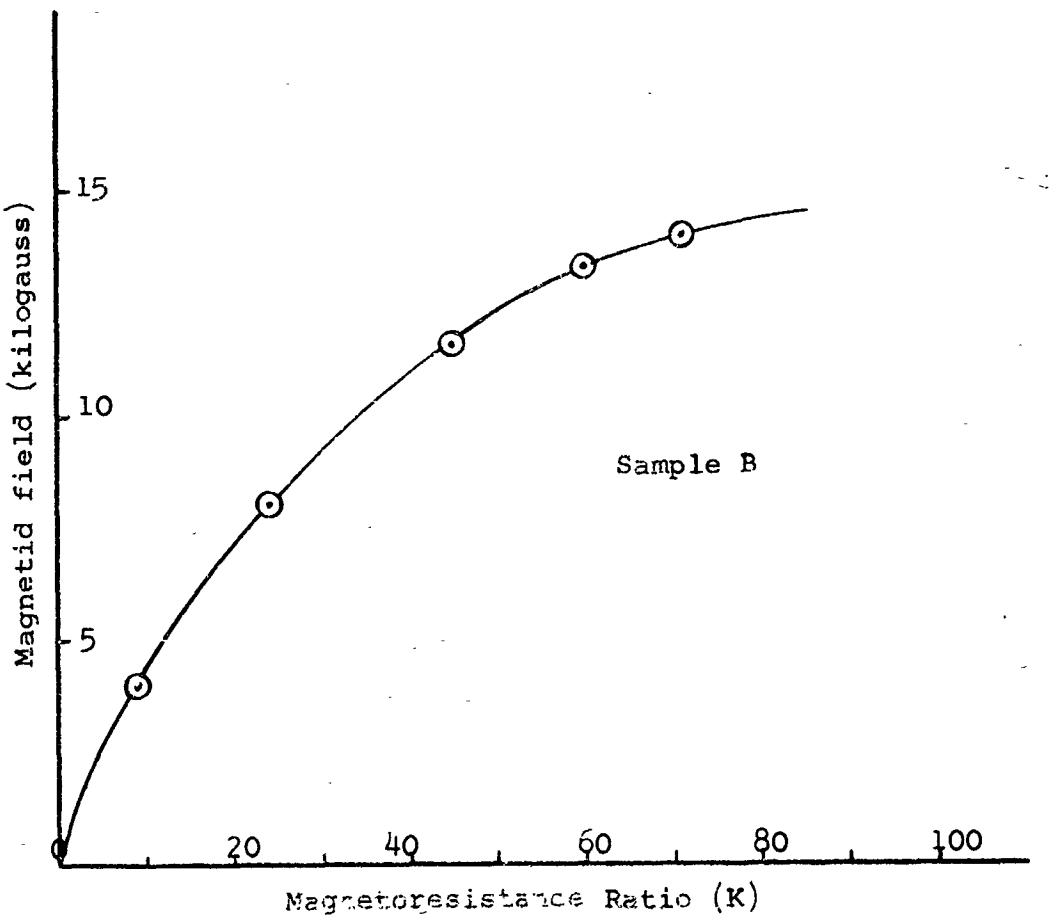
Magnetid field (kilogauss)
15
10
5
Sample B
20
40
60
80
100
Magnetoresistance Ratio (K)

Figure 3.2

further points out the importance of the results obtained for sample A. That is, size for size a corbino disk cannot be made to compare with the sample A configuration as far as current carrying capability, without sacrificing the magnetoresistance ratio.

A maximum K of only 6.7 was measured at 14 kg, as shown in Fig. 3.3.

Sample D and E:

These samples were prepared in order to determine the effect of shorting out the Hall voltage on a bar-type magnetoresistor. Sample E has a lead shunt connected across the sample; and, therefore, it can also be used at superconducting temperatures where the lead would become a perfect shunt. The effect of this shunt resulted in a 40 per cent increase in the magnetoresistance ratio at $80^{\circ}K$ and would undoubtedly show even more at $4.2^{\circ}K$.

A plot of K versus magnetic field is shown in Fig. 3.4 for sample C and Fig. 3.5 for sample D. Notice that the maximum K for sample D was 84.5 at 14 kg, the highest value obtained for all the samples. However, this sample was somewhat larger than sample B, the corbino disk, which could account for some of the difference.

4.0 Experiments at $4.2^{\circ}K$

Because of previously mentioned difficulties with the liquid helium, only two short runs were possible of the several that were planned. One of these involved a corbino magnetoresistor and the other a superconducting coil of niobium wire.

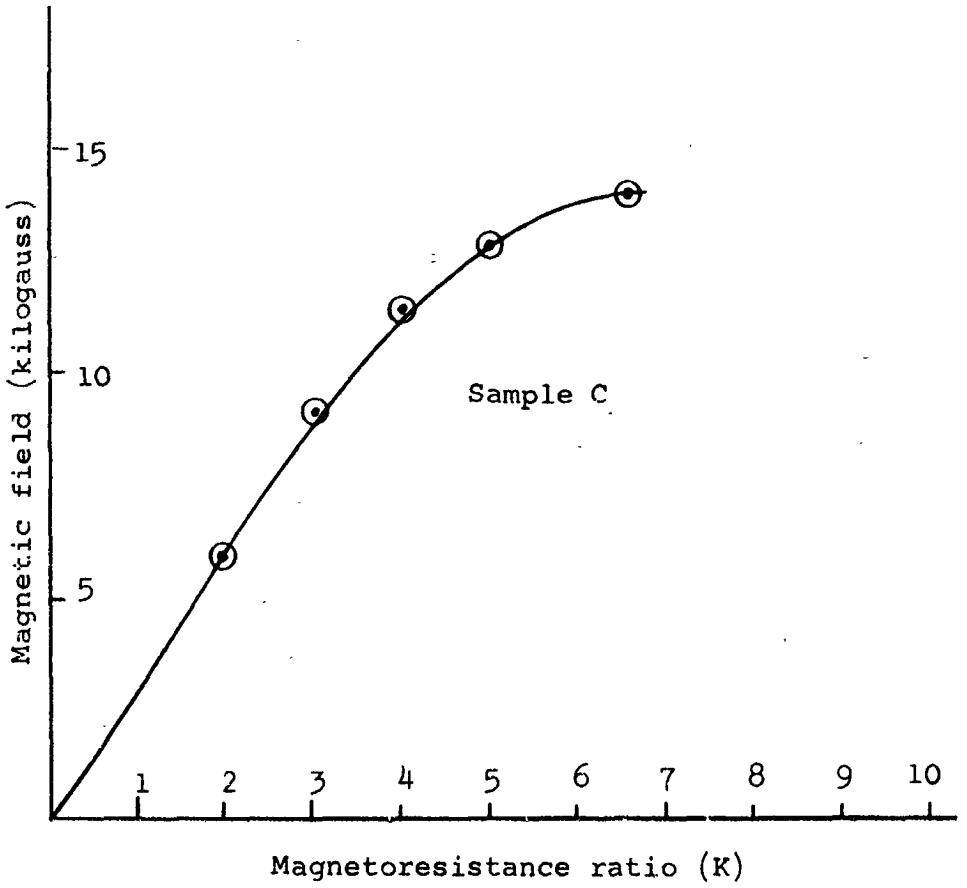
Magnetic field (kilogauss)
15
10
5
Sample C
1
2
3
4
5
6
7
8
9
10
Magnetoresistance ratio (K)

Figure 3.3

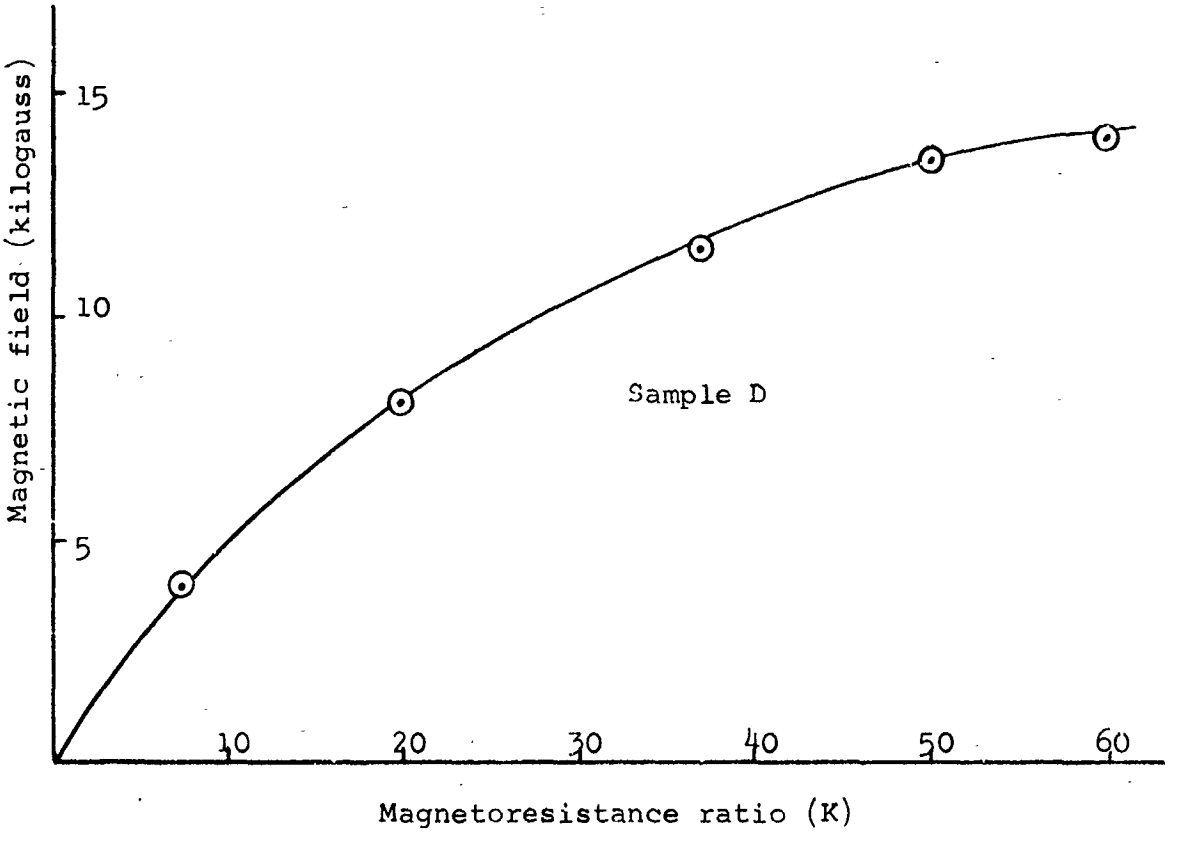
Magnetic field (kilogauss)
15
10
5
Sample D
10
20
30
40
50
60
Magnetoresistance ratio (K)

Figure 3.4

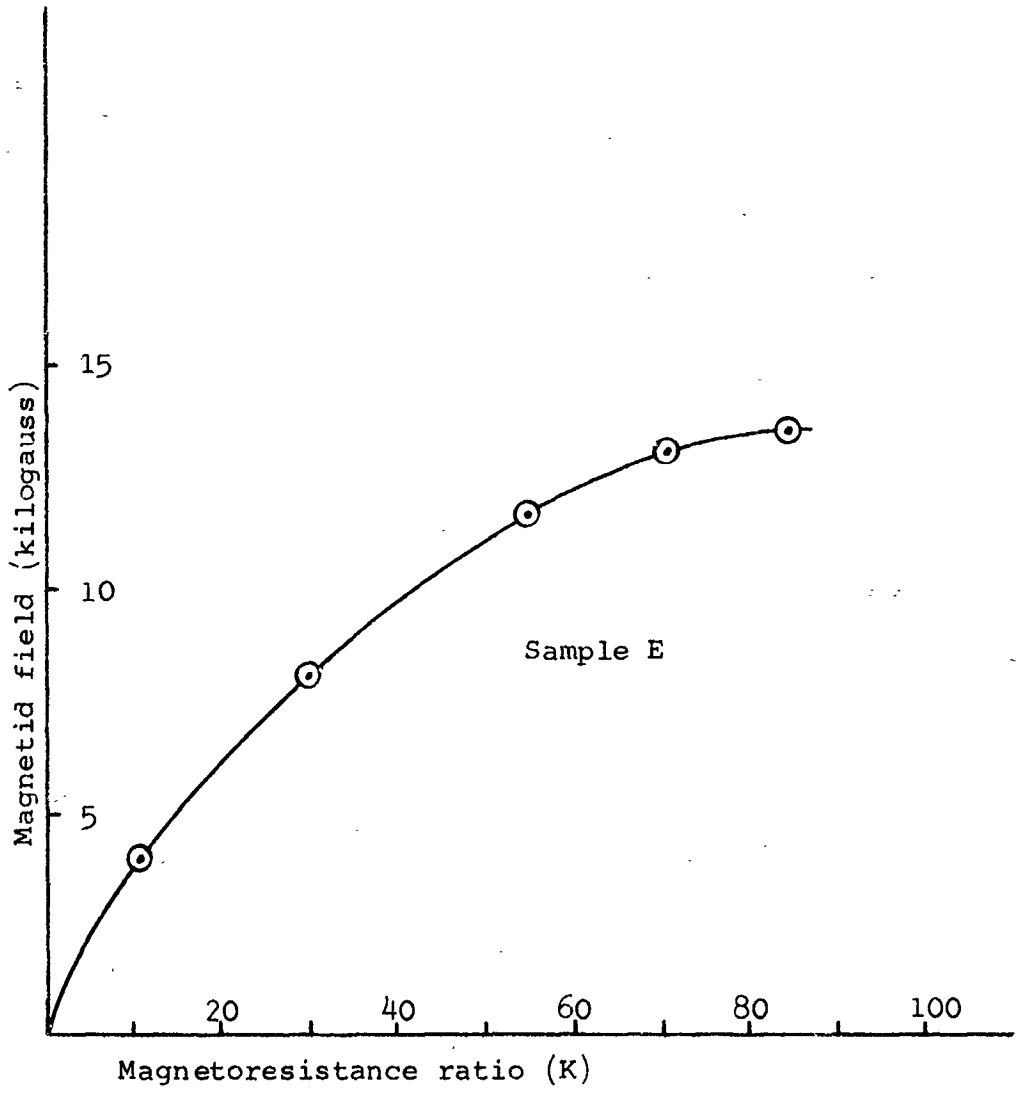
Magnetid field (kilogauss)
15
10
5
Sample E
20
40
60
80
100
Magnetoresistance ratio (K)

Figure 3.5

4.1 Bismuth Corbino Disk at 4.2°K

The test run with a 4 cm diameter corbino (sample B) at 4.2°K was quite encouraging. As shown in Fig. 4.1, a plot of K versus magnetic field, a magnetoresistance ratio of 1000:1 was obtained at a field of only 14 kilogauss. Too, the magnetoresistance had still not saturated at this field.

Of additional interest is the extremely low off-field resistance of this sample--125 micro-ohms. These factors would make this sample suitable in all respects for an inverter system.

4.2 Niobium Coil at 4.2°K

One abbreviated run was made with a coil wound with 160 inches of niobium wire. Use of a modulated field, as described in a previous report,[4] showed some evidence of a switching time that followed 60 cycles; however, no definite conclusions were arrived at on this since the brevity of the run did not permit extensive analysis. However, it was found that the superconductivity to normal transition point could be adequately controlled by either current flow or magnetic field or a combination of same.

4.3 Concluding Remarks on Inverter Possibilities

Considering the high value of K that has been shown to be possible (1000:1 at 14 kg) and the extremely low resistance (125×10^{-6} ohms), it would seem the magnetoresistor could well be adaptable to inverter application. If a square wave magnetic field could be obtained, quite respectable efficiencies could be realized even at field strengths of less than 14 kilogauss.

---

[4] Bechtel, Grannemann, p. 3

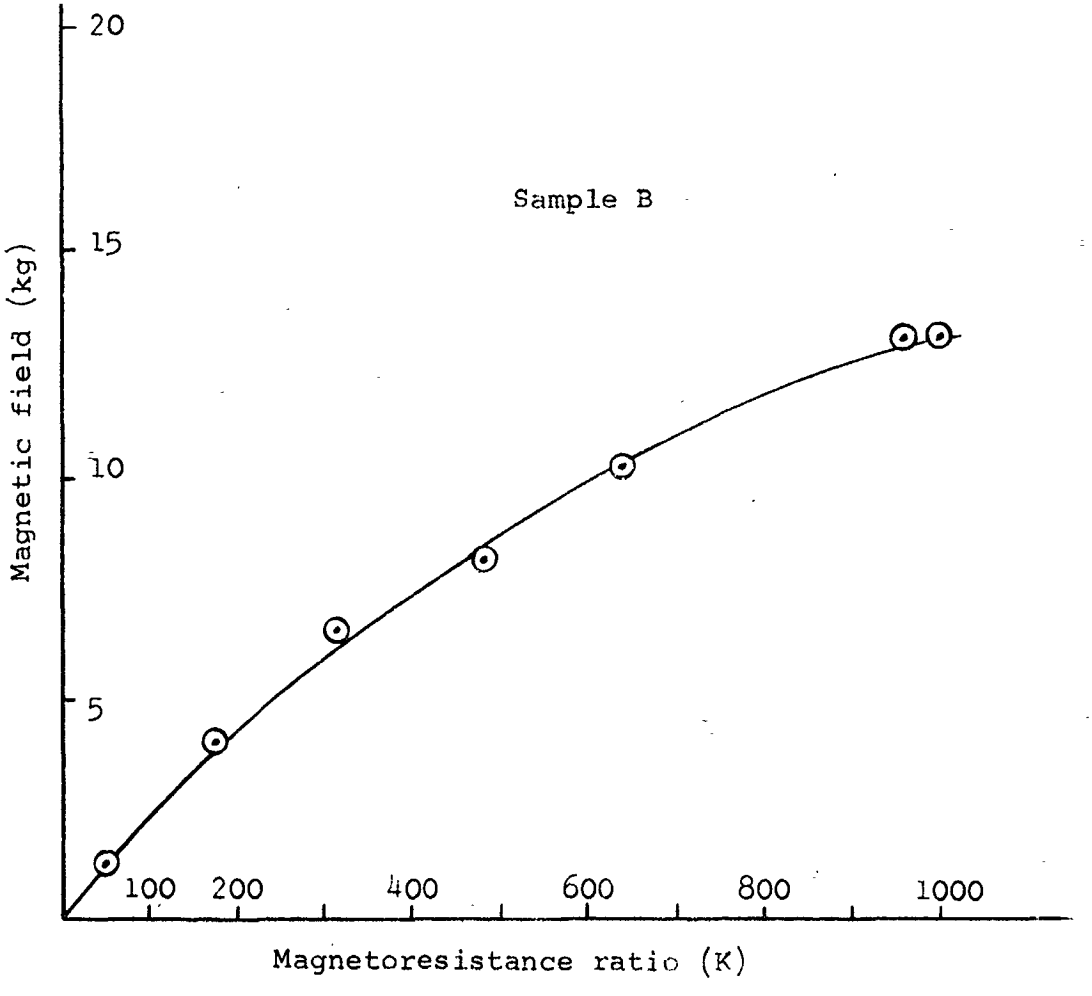
Sample B
Magnetic field (kg)
20
15
10
5
100
200
400
600
800
1000
Magnetoresistance ratio (K)

Figure 4.1

It is probable, however, that the overall efficiency would be unacceptably low if a square wave field is attempted by ordinary means. An idea is being nurtured at this laboratory that could surmount this problem.

This new technique would involve only small I^2R loses and would reduce to negligible the reactive losses and the long inductive rise and fall times. It involves a phenomena of superconductivity that has yet to be exploited as far as is known.

A study to develop this technique is being outlined and will be submitted as a proposal.

5.0 The Multi-Terminal Hall Generator

5.1 Introduction

This chapter describes a study undertaken to maximize the Hall generator efficiency. A mathematical solution is obtained for a multi-terminal Hall generator, and an analytical technique is developed for determining the optimum values of parameters to maximize the generator efficiency.

An equivalent circuit is developed for single output, two output, and N output-terminal Hall generators, and the efficiency expression is obtained as a function of sample dimension, conductivity and Hall coefficient of the material, and magnetic field strength. Some of the results have been checked experimentally with indium antimonide and fields up to 21.5 kilogauss. An efficiency of 40% was obtained experimentally for a nineteen output-terminal Hall generator.

In order to maximize the efficiency, it was found that the mobility, mobility ratio, magnetic field strength, and the number of output-terminal pairs must all be maximized and the impurity concentration must be minimized. It was also found that the optimum load varies proportionally to the half power of N, the number of output pairs.

5.2 Four Terminal Analysis

A Hall generator may be considered as a four-terminal device that uses a magnetic field to couple the input and output. The closest conventional component would be an ideal transformer having a variable turns ratio directly proportional to magnetic field. A Hall generator is a non-reciprocal bilateral device, since both sides of the device may be energized and an output will occur on the opposite side of the device, and its transfer impedances are unequal.

The four terminal model of a one output-terminal Hall generator using proper sign convention of input and output voltage and current for applied magnetic field is shown in Figure 5.1. Two basic equations for voltage and current are:

$$V_A = Z_{11}I_A + Z_{12}I_H \qquad 5.1$$

$$V_H = Z_{21}I_A + Z_{22}I_H \qquad 5.2$$

where Z_{11} is the resistance between the input electrodes when the Hall terminals are open-circuited, and Z_{22} the resistance

between the Hall electrodes when the input is open-circuited. Z_{12} and Z_{21} are the transfer resistances.

$$Z_{11} = \frac{V_A}{I_A}\Bigg|_{I_H = 0}$$

$$Z_{22} = \frac{V_H}{I_H}\Bigg|_{I_A = 0} \qquad 5.3$$

$$Z_{12} = \frac{V_A}{I_H}\Bigg|_{I_A = 0}$$

$$Z_{21} = \frac{V_H}{I_A}\Bigg|_{I_H = 0}$$

These are the impedances we have to consider in a four terminal model of the Hall generator. In Figure 5.1, the input contacts

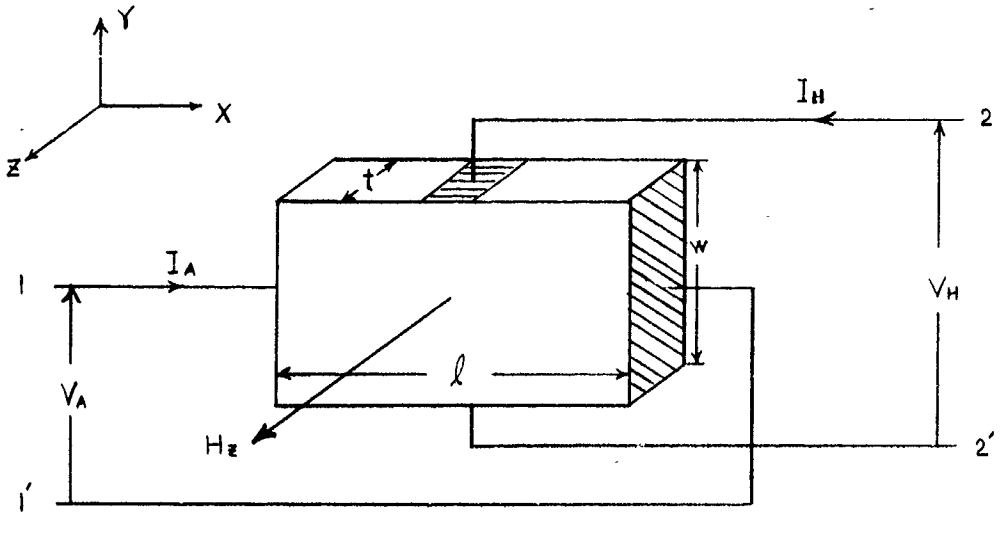

Figure 5.1 Four Terminal Model of the Hall Generator

cover the entire end faces. Input terminals 1 and 1' are energized with the output terminals 2 and 2' left open; then the current density J_A can be written as

$$J_A = \frac{I_A}{Wt} \qquad 5.4$$

where I_A = The total input current in X direction

W = Width of the Hall generator

t = Thickness of the Hall generator

From the relation $J = \sigma E$, and equation 5.4, we get

$$\frac{I_A}{Wt} = \sigma E = \frac{\sigma V_A}{\ell}$$

and

$$Z_{11} = \left.\frac{V_A}{I_A}\right|_{I_H = 0} = \frac{\ell}{\sigma wt} \qquad 5.5$$

where ℓ = Length of the Hall generator

σ = Conductivity of the Hall generator

When current flows in X direction and magnetic field in Z direction, then the Hall voltage is developed in Y direction as shown in Figure 5.1. From the Hall voltage expression, the transfer impedance Z_{21} may be obtained.

$$V_H = \frac{10^{-8} R_H I_A H}{t}$$

$$Z_{21} = \left.\frac{V_H}{I_A}\right|_{I_H = 0} = \frac{10^{-8} R_H H}{t} \qquad 5.6$$

Now, the output terminals 2 and 2' are energized and the input terminals 1 and 1' are left open. In the same way we derived Z_{11}, Z_{22} can be derived,

$$Z_{22} = \left.\frac{V_H}{I_H}\right|_{I_A = 0} = \frac{W}{\sigma t \ell} \qquad 5.7$$

Here we assumed that the output contacts cover the entire end faces. However, Z_{22} for the point contacts of output terminals is usually several times higher than equation 5.7. Modifying equation 5.7, we write

$$Z_{22} = \frac{KW}{\sigma t \ell} \qquad 5.8$$

where K is a multiplication factor depending on the geometry of the slab.

When current flows in minus Y-direction and the magnetic field in Z-direction, then the Hall voltage is developed in minus X-direction differing from the sign convention established in Figure 5.1. Thus

$$V_A = \frac{-10^{-8} R_H H I_H}{t}$$

and

$$Z_{12} = \left.\frac{V_A}{I_H}\right|_{I_A = 0} = \frac{-10^{-8} R_H H}{t} \qquad 5.9$$

A four-terminal equivalent circuit of the Hall generator is shown in Figure 5.2.

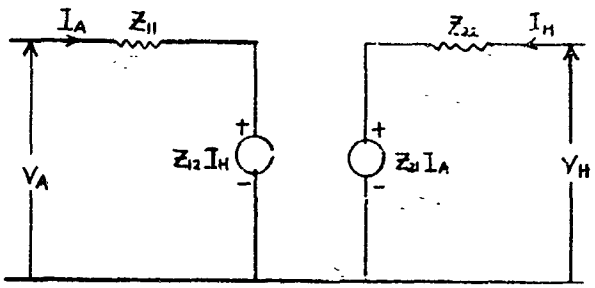

Figure 5.2. Equivalent Circuit of a Four-Terminal Hall Generator

The efficiency of the Hall generator, defined as the ratio of output power to input power, is derived from the equivalent circuit, Figure 5.3.

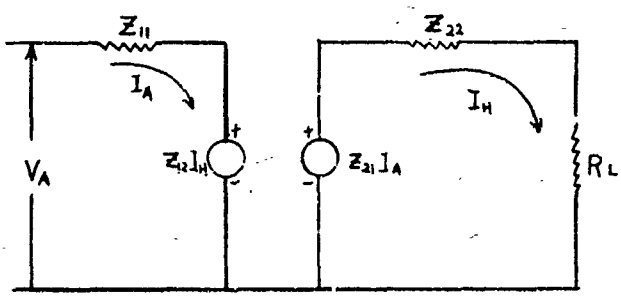

Z_{12} is an absolute value here.

Figure 5.3. Hall Generator Equivalent Circuit with a Load R_L.

Write two loop equations and solve for input and output currents.

$$V_A = Z_{11}I_A + Z_{12}I_H$$

$$0 = -Z_{21}I_A + (Z_{22} + R_L)I_H \qquad 5.10$$

$$I_A = \frac{V_A(Z_{22} + R_L)}{Z_{11}(Z_{22} + R_L) + Z_{12}Z_{21}} \qquad 5.11$$

$$I_H = \frac{V_A Z_{21}}{Z_{11}(Z_{22} + R_L) + Z_{12}Z_{21}} \qquad 5.12$$

The power supplied to the Hall generator P_A and the power output P_o are

$$P_A = V_A I_A = \frac{V_A^2(Z_{22} + R_L)}{Z_{11}(Z_{22} + R_L) + Z_{21}^2} \qquad 5.13$$

$$P_o = I_H^2 R_L = \frac{V_A^2 Z_{21}^2 R_L}{Z_{11}(Z_{22} + R_L) + Z_{21}^2} \qquad 5.14$$

The efficiency, η, of the Hall generator with one output can be obtained from equation 5.13 and 5.14.

$$\eta = \frac{P_o}{P_A} = \frac{Z_{21}^2 R_L}{(Z_{22} + R_L)\left[Z_{11}(Z_{22} + R_L) + Z_{21}^2\right]} \qquad 5.15$$

Substituting the Hall generator parameters in equation 5.15, we get the efficiency expression in terms of sample dimensions,

Hall constant, conductivity and magnetic field.

$$\eta = \frac{(10^{-8}R_H)^2 \sigma t W \ell R_L}{(KW + \sigma t \ell R_L)\left[KW + \sigma t \ell R_L + (10^{-8}R_H\sigma)^2 W\right]} \qquad 5.16$$

where:

$R = \frac{3\pi}{8nec}$, Hall constant in cm^3/coulomb.

H = Magnetic field in gauss

σ = Conductivity of the sample when the magnetic field H is perpendicular to the current, in mho-cm^{-1}

K = Multiplication factor of Z_{22}

t = Thickness of the sample in cm

W = Width of the sample in cm

ℓ = Length of the sample in cm

R_L = Load resistance in ohms.

5.3 Six Terminal Analysis

A Hall generator with two output-terminal pairs may be treated as a six terminal network (see Figure 5.4).

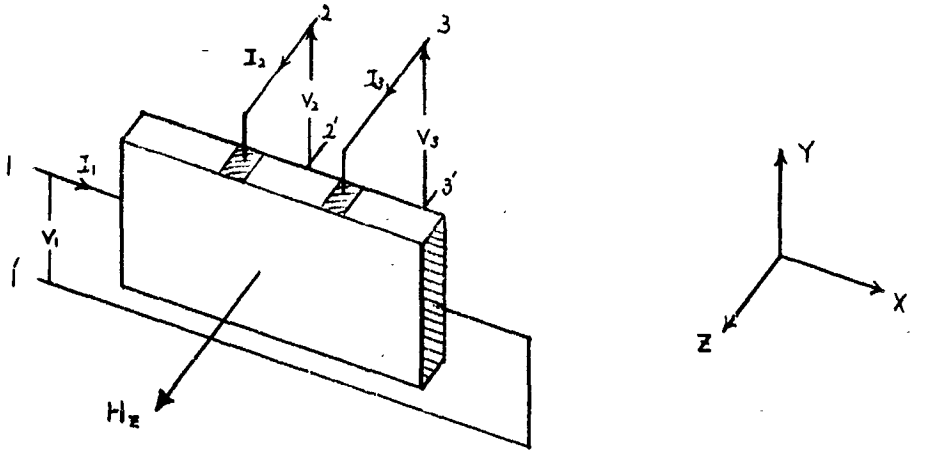

Figure 5.4. Six Terminal Model of the Hall Generator

The voltage and current equations for six terminal network shown in Figure 5.4 are

$$V_1 = Z_{11}I_1 + Z_{12}I_2 + Z_{13}I_3 \qquad 5.17$$

$$V_2 = Z_{21}I_1 + Z_{22}I_2 + Z_{23}I_3 \qquad 5.18$$

$$V_3 = Z_{31}I_1 + Z_{32}I_2 + Z_{33}I_e \qquad 5.19$$

where Z_{11}, Z_{22} and Z_{33} are driving point impedances, and Z_{12}, Z_{21}, Z_{13}, Z_{31} are transfer impedances. Z_{23} and Z_{32} may be called coupling impedances between two output terminals. With the same analysis as we did for a four terminal network in the previous section, we can easily derive the following impedance equations.

$$Z_{11} = \frac{V_1}{I_1}\Bigg|_{I_2=I_3=0} = \frac{\ell}{\sigma t w}$$

$$Z_{12} = \frac{V_1}{I_2}\Bigg|_{I_1=I_3=0} = \frac{-10^{-8}R_H}{t}$$

$$Z_{13} = \frac{V_1}{I_3}\Bigg|_{I_1=I_2=0} = \frac{-10^{-8}R_H}{t}$$

$$Z_{21} = \frac{V_2}{I_1}\Bigg|_{I_2=I_3=0} = \frac{10^{-8}R_H}{t}$$

$$Z_{22} = \frac{V_2}{I_2}\Bigg|_{I_1=I_3=0} = \frac{KW}{\sigma t \ell}$$

$$Z_{31} = \frac{V_3}{I_1}\Bigg|_{I_2=I_3=0} = \frac{10^{-8} R_H}{t} \qquad 5.20$$

$$Z_{33} = \frac{V_3}{I_3}\Bigg|_{I_1=I_2=0} = \frac{KW}{\sigma t \ell}$$

The theoretical derivation of the coupling impedances, Z_{23} and Z_{32}, is very complicated. Z_{23} is defined by $Z_{23} = \frac{V_2}{I_3}\Big|_{I_1=I_2=0}$ which is the ratio of the voltage induced across the output terminals 2 and 2' due to the current I_3. When current I_3 flows through the sample as shown in Figure 5.1, the electric field will be developed in minus Y direction.

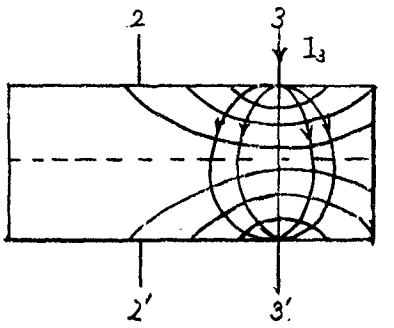

Figure 5.5. Equipotential Lines

The equipotential lines intersecting perpendicularly the electric field lines may be drawn as Figure 5.5. As the internal resistance measured across the output terminal is so small that usually very small voltage drop occurs by the current flowing through terminal 3-3', and a small potential difference is measureable across the terminal 2-2'. The values of Z_{23} and Z_{32} are determined by experiment in this study.

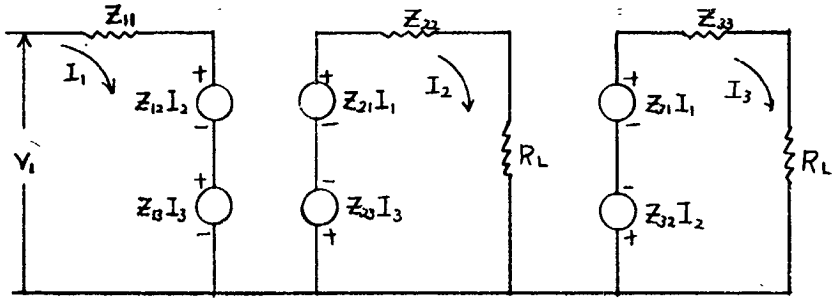

Figure 5.6. Equivalent Circuit of the Six-Terminal Hall Generator

Currents I_1, I_2 and I_3 can be derived from the equivalent circuit, Figure 5.6, by writing loop equations

$$V_1 = Z_{11}I_1 + Z_{12}I_2 + Z_{13}I_3$$

$$0 = -Z_{21}I_1 + (Z_{22} + R_L)\, I_2 + Z_{23}I_3 \qquad 5.21$$

$$0 = -Z_{31}I_1 + Z_{32}I_2 + (Z_{33} + R_L)\, I_3$$

Solving for I_1, I_2 and I_3, we get

$$I_1 = \frac{V_1\left[(Z_{22} + R_L)^2 - Z_{23}^2\right]}{\left[(Z_{22} + R_L) - Z_{23}\right]\left[Z_{11}(Z_{22} + R_L) + 2Z_{21}^2\right]}$$

$$= \frac{V_1(Z_{22} + R_L + Z_{23})}{Z_{11}(Z_{22} + R_L + Z_{23}) + 2Z_{21}^2} \qquad 5.22$$

$$I_2 = \frac{V_1 Z_{21}}{Z_{11}(Z_{22} + R_L + Z_{23}) + 2Z_{21}^2} \qquad 5.23$$

$$I_3 = \frac{V_1 Z_{21}}{Z_{11}(Z_{22} + R_L + Z_{23}) + 2Z_{21}^2} \qquad 5.24$$

The output currents, I_2 and I_3, are equal since equal Hall voltages are developed across each output terminal, assuming that the length to width ratio is greater than five and the loads are the same. The total power output is the sum of the powers delivered to each load, P_{01} and P_{02}. The power supplied to the Hall generator P_A and the power output P_{01} and P_{02} are:

$$P_A = \frac{V_1^2(Z_{22} + R_L + Z_{23})}{Z_{11}(Z_{22} + R_L + Z_{23}) + 2Z_{21}^2} \qquad 5.25$$

$$P_{01} = \frac{V_1^2 Z_{21}^2 R_L}{\left[Z_{11}(Z_{22} + R_L + Z_{23}) + 2Z_{21}^2\right]^2} \qquad 5.26$$

$$P_{02} = \frac{V_1^2 Z_{21}^2 R_L}{\left[Z_{11}(Z_{22} + R_L + Z_{23}) + 2Z_{21}^2\right]^2} \qquad 5.27$$

$$P_{total} = P_{01} + P_{02} = \frac{2V_1^2 Z_{21}^2 R_L}{\left[Z_{11}(Z_{22} + R_L + Z_{23}) + 2Z_{21}^2\right]^2} \qquad 5.28$$

The efficiency of the two output-terminal Hall generator is the ratio of total power out to power delivered to the generator

$$\eta = \frac{P_{total}}{P_A}$$

$$= \frac{2Z_{21}^2 R_L}{(Z_{22} + R_L + Z_{23})\left[Z_{11}(Z_{22} + R_L + Z_{23}) + 2Z_{21}^2\right]} \qquad 5.29$$

The efficiency in terms of the Hall generator parameters is given by the equation

$$\eta = \frac{2(10^{-8}R_H)^2 \sigma^3 tW\ell R_L}{\left[KW + \sigma t\ell(R_L + Z_{23})\right]\left[KW + \sigma t\ell(R_L + Z_{23}) + 2W(10^{-8}R_H\sigma)^2\right]} \qquad 5.30$$

5.4 Multiterminal Analysis

In sections 5.2 and 5.3, we have analyzed the Hall generator with one output-terminal and two output-terminals. From those previous analyses, an equation for a general N output-terminal Hall generator will be derived in this section. Figure 5.7 shows a N output-terminal Hall generator.

All output terminals are equally spaced, and direction of the input current I_1, and magnetic field H_z are in the X and Z directions respectively. Assuming length of the Hall generator is five times greater than width of the sample, the Hall voltages developed across each output are the same except at the terminals at each end due to the shorting effect by input terminal contacts.

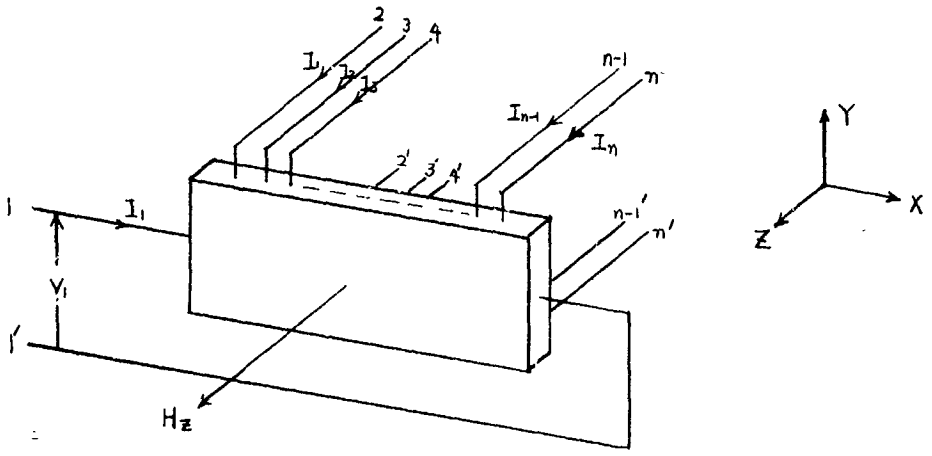

Figure 5.7. N Output-Terminal Hall Generator

When the loads are connected across each output terminal, Hall currents will flow through the load and back to the sample in such a direction that a voltage will be induced across the input terminal (in positive direction) by the relation of $V_H = \frac{R_H H I_H}{t}$, where I_H is the Hall current, R_H is the Hall constant, H is the magnetic field, t is the thickness and V_H is the induced Hall voltage across the input-terminal due to the Hall current I_H. If the resistance of the loads are all the same,

all output currents would be the same, as the Hall voltages across each load are the same. Therefore, the total voltage induced across the input terminal by Hall current is the sum of voltages induced by individual output Hall currents.

N equations may be derived for an N terminal device and an equivalent circuit can be developed (See Figure 5.8). The N equations are:

$$\begin{aligned} V_1 &= Z_{11}I_1 + Z_{12}I_2 + Z_{13}I_3 + \text{-----} + Z_{1n}I_n \\ V_2 &= Z_{21}I_1 + Z_{22}I_2 + Z_{23}I_3 + \text{-----} + Z_{2n}I_n \\ V_n &= Z_{n1}I_1 + Z_{n2}I_2 + Z_{n3}I_3 + \text{-----} + Z_{nn}I_n \end{aligned} \qquad 5.31$$

We may write the Z parameters in a matrix form.

$$\begin{vmatrix} Z_{11} & Z_{12} & \text{----------} & Z_{1n} \\ Z_{21} & Z_{22} & \text{----------} & Z_{2n} \\ Z_{31} & Z_{32} & \text{----------} & Z_{3n} \\ Z_{n1} & Z_{n2} & \text{----------} & Z_{nn} \end{vmatrix} \qquad 5.32$$

The impedances in the first column of the matrix except Z_{11} are transfer impedances, and they are all the same.

$$Z_{21} = Z_{31} = \text{----------} Z_{n1} = \frac{10^{-8} R_H H}{t} \qquad 5.33$$

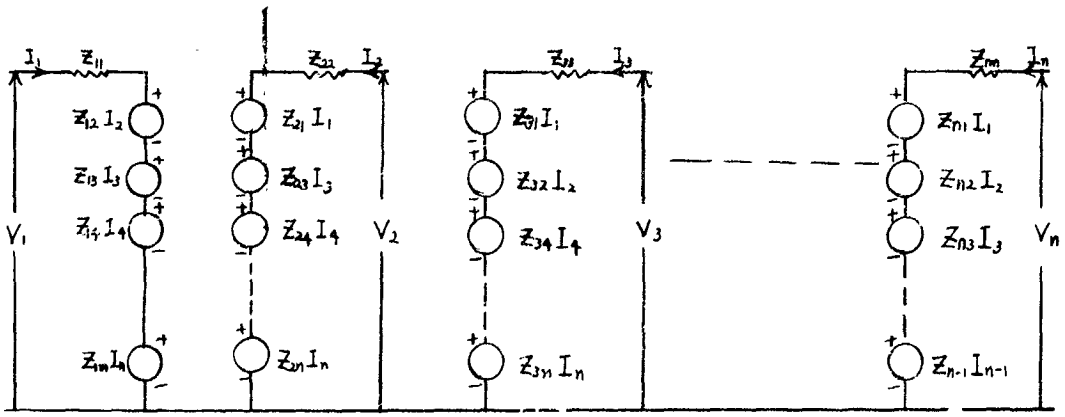

(a)

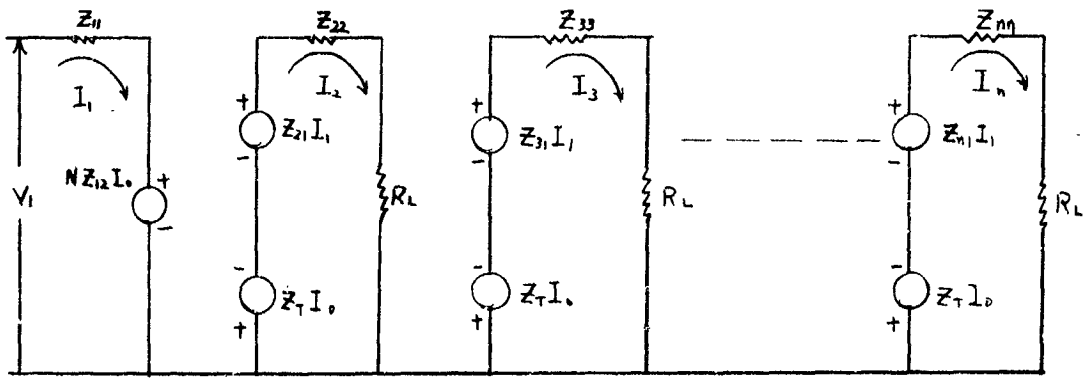

(b)

Fig. 5.8 Equivalent Circuit of an N Output-Terminal Hall Generator.
a) without loads. b) with loads.

Also the impedances in the first row of the matrix except Z_{11} are the same.

$$Z_{12} = Z_{13} = \cdots\cdots\cdots Z_{1n} = \frac{-10^{-8} R_H H}{t} \qquad 5.34$$

Z_{11} is a driving point impedance at the input terminal when all output terminals are open circuited and has the same expression as equation 5.5.

$$Z_{11} = \frac{\ell}{\sigma w t} \qquad 5.35$$

Z_{nn} (n=2, 3, --- n) impedances are the driving point impedances at each output terminal with all terminals left open, and they are all the same.

$$Z_{nn} = \frac{KW}{\sigma t \ell} \quad , \; n=2, \; 3, \; \cdots \; n \qquad 5.36$$

The rest of the impedances in the matrix are coupling impedances between output terminals and depend on the relative distance between coupling terminals. The coupling impedance Z_{mn} is negligible when m and n differ more than 3 for a narrow rectangular slab, and they were measured experimentally.

Now we can simplify equation 5.31 by lumping all the same parameters and letting all output currents be I_o (See Figure 5.8-b).

$$\begin{aligned} V_1 &= Z_{11} I_1 + N Z_{12} I_o \qquad N = n-1 \\ V_2 &= Z_{21} I_1 + (Z_{22} + Z_T)\, I_2 \\ V_n &= Z_{n1} I_1 + (Z_{nn} + Z_T)\, I_n \end{aligned} \qquad 5.37$$

where Z_T is the sum of all coupling impedances and

$I_o = I_2 = I_3 \text{ ------- } = I_n$.

Figure 5.8-b is an equivalent circuit of an n terminal Hall generator with the load R_L connected across each output terminal. Since the output loops are all alike, only input and one output loop equations are derived here.

$$V_1 = Z_{11}I_1 + NZ_{12}I_o \tag{5.38}$$

$$0 = -Z_{21}I_1 + (Z_{22} + R_L + Z_T)\, I_2 \tag{5.39}$$

Solving for I_1 and I_2, we have

$$I_1 = \frac{V_L(Z_{22} + R_L + Z_T)}{Z_{11}(Z_{22} + R_L + Z_T) + NZ_{12}^2} \tag{5.40}$$

$$I_2 = \frac{V_1 Z_{21}}{Z_{11}(Z_{22} + R_L + Z_T) + NZ_{12}^2} \tag{5.41}$$

The power applied to the Hall generator is then

$$P_{in} = V_1 I_1 = \frac{V_1^2\,(Z_{22} + R_L + Z_T)}{Z_{11}(Z_{22} + R_L + Z_T) + NZ_{12}^2} \tag{5.42}$$

and the power delivered to the output terminal 2 is

$$P_{02} = I_2^2\, R_L = \frac{V_1^2\, Z_{21}^2\, R_L}{\left[Z_{11}(Z_{22} + R_L + Z_T) + NZ_{12}^2\right]^2} \tag{5.43}$$

The total power available to the loads is the sum of the power delivered to N loads.

$$P_{OT} = I_2^2 R_L + I_3^2 R_L + \text{----------} I_n^2 R_L$$

$$= N I_o^2 R_L$$

$$= \frac{N V_1^2 Z_{21}^2 R_L}{\left[Z_{11}(Z_{22} + R_L + Z_T) + N Z_{12}^2\right]^2} \qquad 5.44$$

The efficiency of the N output Hall generator is the ratio of the total power output to the power supplied to the Hall generator.

$$\eta_n = \frac{P_{OT}}{P_{in}} = \frac{N Z_{21}^2 R_L}{(Z_{22}+R_L+Z_T)\left[Z_{11}(Z_{22}+R_L+Z_T) + N Z_{12}^2\right]} \qquad 5.45$$

The efficiency in terms of Hall generator parameters is obtained in equation 5.46.

$$\eta_n = \frac{N(10^{-8} R_H H)^2 R_L \sigma^3 t W \ell}{\left[KW+\sigma t \ell (R_L+Z_T)\right]\left[KW+\sigma t \ell (R_L+Z_T) + NW(10^{-8} R_H H \sigma)^2\right]} \qquad 5.46$$

where:

R_H = $\frac{3\pi}{8nec}$, Hall constant in cm^3/coulomb

H = Magnetic field in gauss

σ = Conductivity of a sample in mhos/cm

K = Multiplication factor of Z_{22}

t, W, ℓ = Thickness, width, length of a sample in cm

R_L = Load in ohms

If the output terminals are shorted, $R_L = 0$, we may get an input voltage expression in terms of the number of output terminals shorted from equation 5.38 and equation 5.39.

$$V_1 = Z_{11}I_1 + \frac{NZ_{12}^2}{(Z_{22} + Z_T)} I_1$$

$$= V_c + SN \qquad 5.47$$

where V_o is the input voltage with all output terminals open-circuited, and S is a proportionality constant. Equation 5.47 shows that the input voltage is directly proportional to the number of outputs shorted for constant applied current and magnetic field, resulting in increase of the input resistance of the Hall generator. The magnetoresistance of a semiconductor is defined as the ratio of resistance of the material with magnetic field perpendicular to the current to the resistance of the material without magnetic field. Hence, the magnetoresistance is increased by increasing the number of terminals which short the Hall voltage along the material. The theoretical and experimental curves for voltage input versus number of output terminals shorted at room temperature is shown in Figure 5.9.

5.5 Optimizing the Parameters for Maximum Efficiency

From the expression for the efficiency, we are able to determine the optimum operating conditions and the ideal material parameters for the Hall generator. In principle, a set of

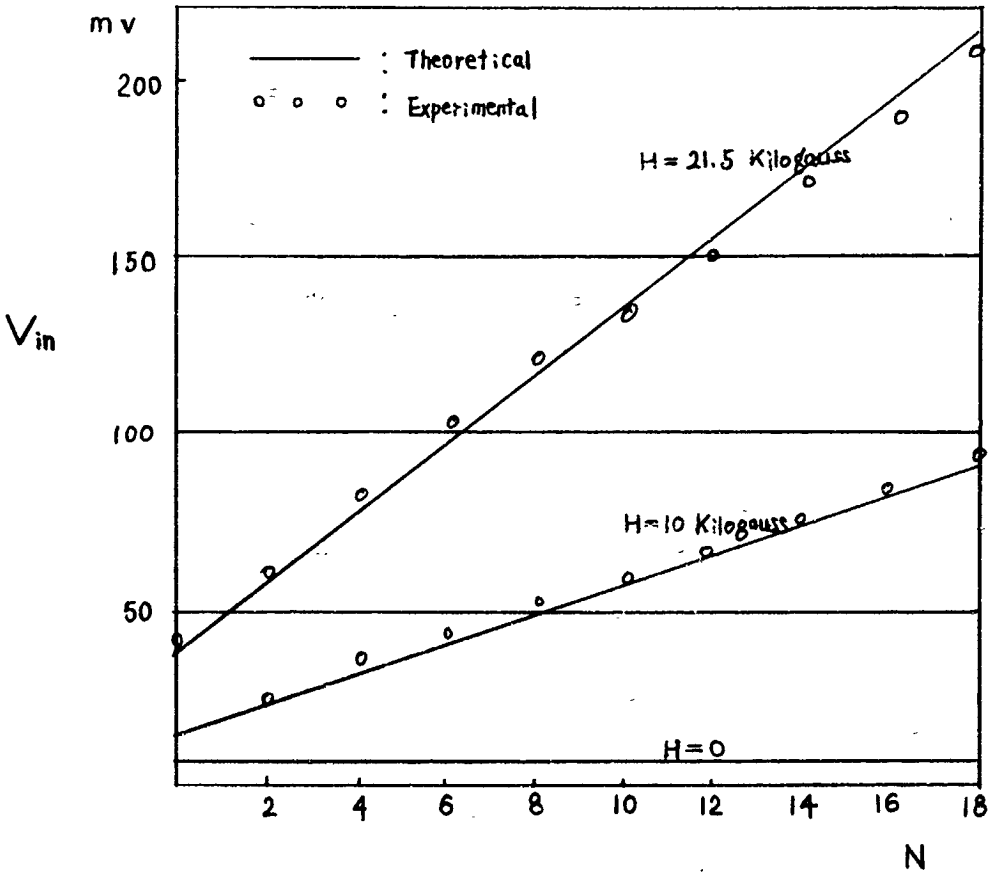

Fig. 5.9 Input Voltage Variation with Number of Output-Terminals Shorted.

simultaneous equations can be obtained by partial differentiation of equation 5.16 with respect to all the variables.

At first, the optimum load R_L for which the efficiency of the Hall generator becomes maximum is derived. For simplicity of calculation, equation 5.15 is differentiated with respect to R_L, and the optimum value of the load is derived here.

$$R_{Lo} = z_{22}\sqrt{1 + \frac{z_{21}^2}{z_{11}z_{22}}} \approx z_{22} \qquad 5.48$$

Since Z_{21} is smaller than both Z_{11} and Z_{22}, we may take the optimum load as equal to Z_{22}. Substituting this value in equation 5.15, we obtain

$$\eta_{max} = \frac{z_{12}^2}{2\left[2z_{11}z_{22} + z_{12}^2\right]}$$

$$= \frac{1}{2\left[\frac{2z_{11}z_{22}}{z_{12}^2} + 1\right]} \qquad 5.49$$

where

$$\frac{2z_{11}z_{22}}{z_{12}^2} = \frac{2K}{(10^{-8} R_H H\sigma)^2}$$ in terms of Hall generator parameters.

The efficiency can be increased by making the quantity $\frac{2K}{(10^{-8}R_H H\sigma)^2}$ as small as possible, that is $R_H\sigma H$ has to be large. If we substitute $R_H = \frac{3\pi}{8}\frac{\mu}{\sigma}$, in the above expression, then

$$R_H\sigma H = \frac{3\pi}{8}\mu H \qquad 5.50$$

Equation 5.50 indicates that higher mobility and magnetic fields are required for higher efficiency.

The Hall coefficient in terms of carrier concentration and mobility ratio is

$$R_H = \frac{-3\pi}{8}\frac{nb^2 - p}{(nb + p)^2} \qquad 4.50$$

R_H is high for a material with high mobility ratio b and low impurity concentration p for n-type material.

The optimum conditions for single output-terminal Hall generator would hold for a multi-terminal Hall generator except the optimum load, which is directly proportional to the one half power of N, number of output terminal pairs, for a given sample dimensions and magnetic field. The optimum load, R_{Lo}, of an N output-terminal Hall generator is found by differentiating equation 5.45 with respect to R_L.

$$R_{Lo} \approx \sqrt{z_{22}^2 + \frac{Nz_{12}^2 z_{22}}{z_{11}}}$$

$$\approx z_{12}\sqrt{\frac{Nz_{22}}{z_{11}}} = \frac{10^{-8}R_H HW}{t\ell}\sqrt{KN} \qquad 5.51$$

for $N > 50$

Substituting equation 5.51 in equation 5.46, the maximum efficiency is obtained.

$$\eta_{max} = \frac{(10^{-8} R_H H\sigma)^3 K^{1/2} N^{3/2}}{\left[K + (10^{-8}RH\sigma)K^{1/2}N^{1/2}\right]\left[K + (10^{-8}RH\sigma)^{1/2}N^{1/2} + (10^{-8}RH\sigma)^2 N\right]} \qquad 5.52$$

where Z_T is neglected.

The efficiency goes to one at the limit of N,

$$\lim_{N\to\infty} \eta = \frac{(10^{-8}RH\sigma)^3 K^{1/2}}{(10^{-8}RH\sigma)K^{1/2}(10^{-8}RH\sigma)^2} = 1$$

The optimum operating conditions and the ideal material parameters for the Hall generator are:

1) High mobility
2) Low impurity concentration
3) High mobility ratio
4) High magnetic field
5) Large number of output-terminal pairs

5.6 Experimental Results

The Hall generator used in the experiments was a thin slice cut from a large ingot of InSb. The mobility and conductivity at the room temperature are 65,000 cm^2/volt-sec and 200 mhos/cm respectively. The magnetic field of 21.5 kilogauss and the input current of 10 milliampere were used for the experiment.

The conductivity of the sample was found experimentally by measuring the voltage drop across the sample, keeping the input current constant at 10 milliamperes for different temperatures and magnetic fields. The experimental values were plotted and compared with the theoretical values[6] in Figure 5.10 and Figure 5.11.

Figure 5.9 is a curve of the input terminal voltage against N, the number of outputs shorted, at different fields. When the field is zero, the input voltages do not vary with N. When a field is applied, the input voltage varies proportionally with N, and with higher fields the slope is steeper. This indicates that the input resistance is greatly increased by shorting the output.

Before the output is shorted, the electric fields due to the charges accumulated on the edges of the sample equals the Lorentz force exerted on the electrons, resulting in current density lines being parallel to the edges of the sample. After the outputs are shorted, the charges flow through the shorts and unequalize the Lorentz force. Thus the current density lines are bent at those regions where the output is shorted as shown in Figure 5.12.

---

[6]The theoretical values were calculated from the equations derived by David L. Endsley and W. W. Grannemann. "A Theoretical and Experimental Analysis of a Hall Generator" TREE-27, Engineering Experiment Station, University of New Mexico, pp. 13-16, 1959.

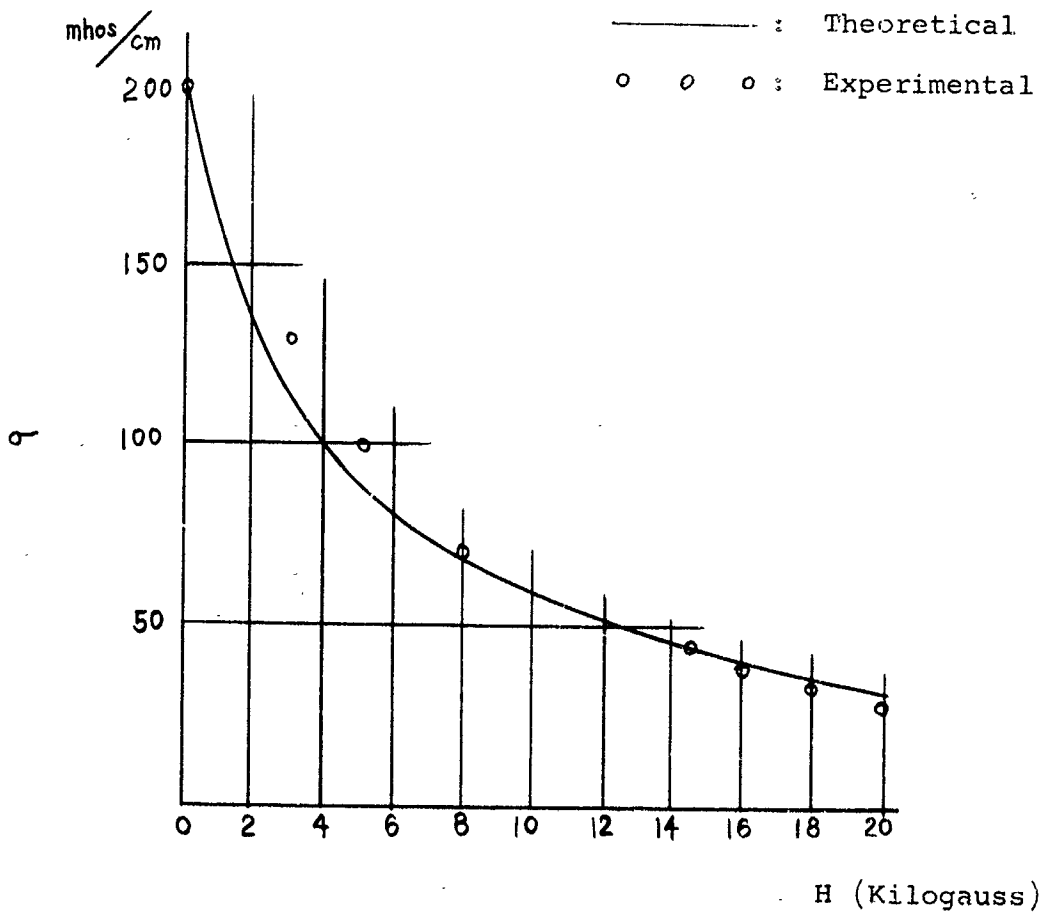

Fig. 5.10 Variation of Conductivity with Magnetic Field for InSb.

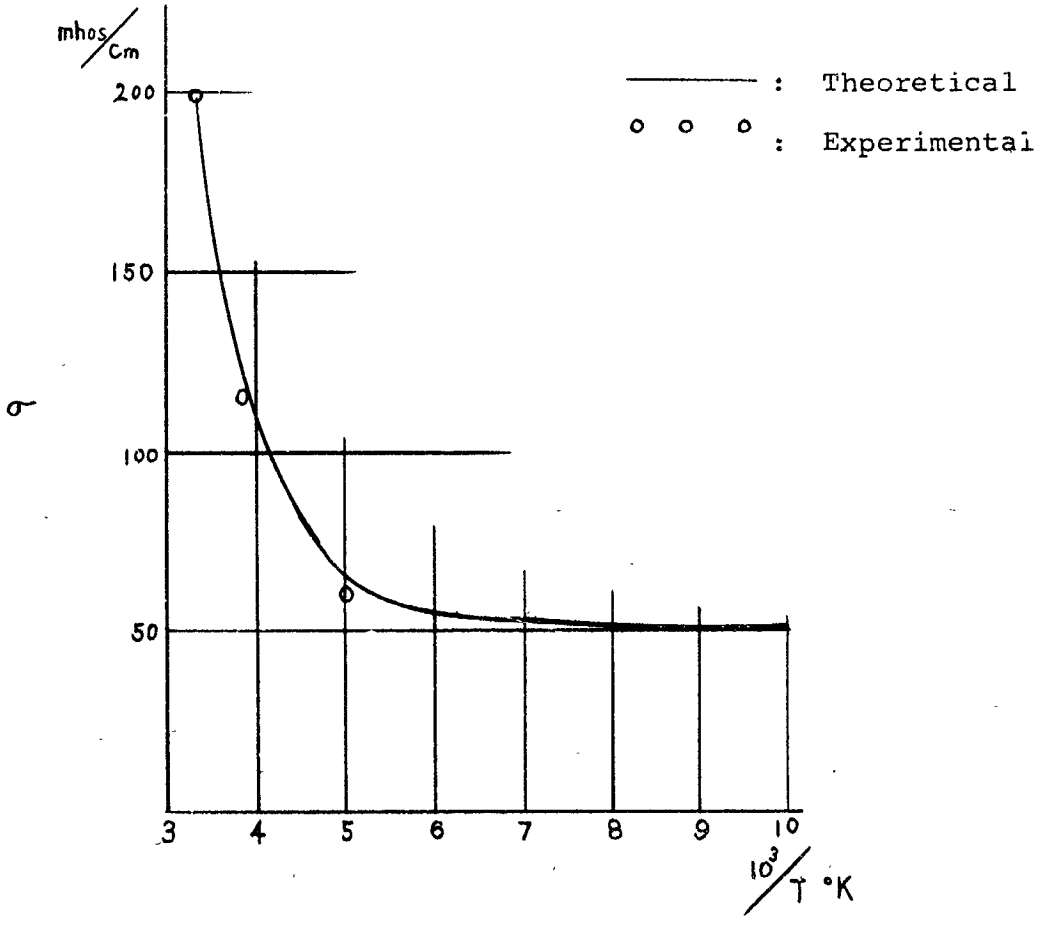

Fig 5.11 Theoretical and Experimental Temperature Dependence of Conductivity for InSb.

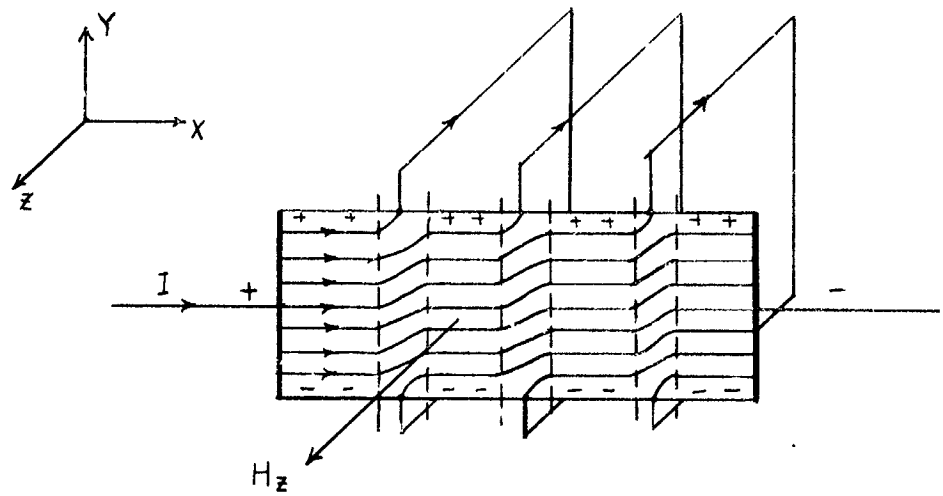

Figure 5.12. Hall Generator with Outputs Shorted

When the current lines bend, the carriers have to travel a longer path in the device. At the same time the current component in the Y direction produces a force opposing the carrier drift in X direction. These effects increase the resistance of the Hall device.

Nineteen output terminals were connected on the InSb slab of length 2.5 cm, width 0.5 cm., and thickness 0.044 cm., and the efficiency was measured experimentally for a different number of outputs. The multiple factor K in Z_{22} of 16 and the total coupling resistance Z_T of .5 ohm were obtained experimentally. The experimental efficiency values are plotted and compared with theoretical values in Figure 5.13.

1) Theoretical curve when the load is optimized for each N.

2) Theoretical curve when the load is optimized for N = 19.

R_L = 9 ohms.

3) Experimental curve for case 2), (R_L = 9 ohms)

H = 21.5 kilogauss

I_{in} = 10 m.a.

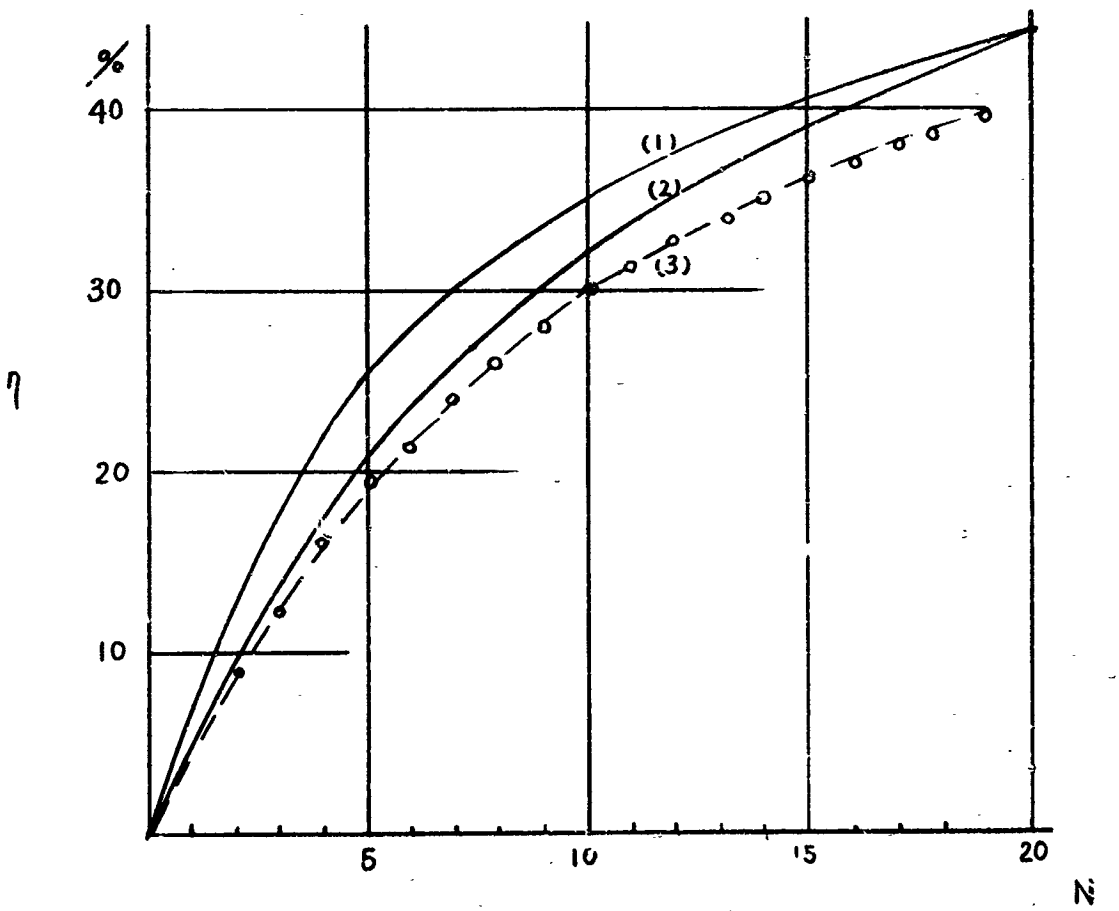

Fig. 5.13 Efficiency Variation with the Number of Output Pairs.

5.7 Summary and Conclusions

In order to analyze a multi-terminal Hall generator, at first an equivalent circuit was developed for a single output Hall generator and treated as a four-terminal network. The efficiency equation is derived from the equivalent circuit in terms of the circuit parameters which are dependent on the dimension of the sample, characteristics of the material used, and magnetic field.

Next, a two output-terminal Hall generator was analyzed by treating it as a six-terminal network. Finally, a general equivalent circuit was developed for the N output terminal Hall generator.

In developing an equivalent circuit of an N output-terminal Hall generator, a few assumptions were made: the Hall voltages are the same at all outputs; the voltages developed due to misalignment of the output contacts are very small; and the output currents are all the same. Also, the coupling impedances between output terminals, Z_{mn}, are determined experimentally and lumped in one parameter, Z_T.

The optimum values of parameters in the efficiency equation were determined analytically and some of them were verified by experiment. These optimum conditions for maximum efficiency are:

1) High mobility
2) Low impurity concentration

3) High mobility ratio

4) High magnetic field

5) Large number of output terminal pairs

The experimental values are accurate to within 10%. The maximum efficiency of 40% for 19 output terminals was obtained experimentally. This can be increased to about 60% by increasing the number of output-terminal to one hundred.

The multi-terminal Hall generator may be used as a DC to AC inverter by applying an alternating magnetic field.

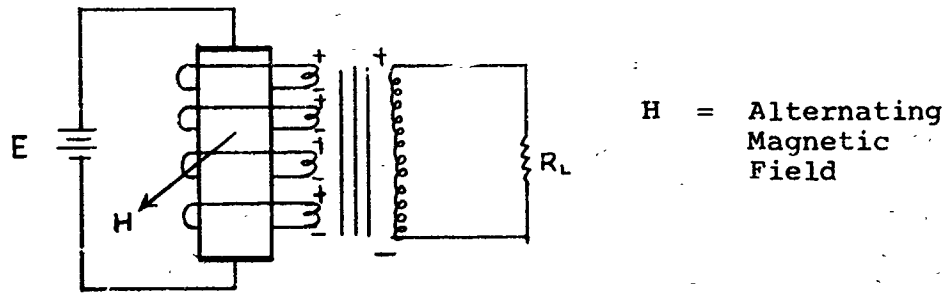

Figure 5.14 Hall Generator as a DC to AC Inverter

As shown in Figure 5.14, the output terminals of the Hall generator are connected to the primary coils of a transformer, of which the secondary coil is connected to a load R_L. Each

primary coil induces a voltage across the secondary coil so that the total voltage developed across the secondary coil is the sum of voltages developed by each primary coil. The maximum efficiency will be obtained by choosing the load properly such that the impedance looking into each primary coil satisfies the optimum load condition described earlier.